Find the rocks and the fluids will follow — AVO as a tool for lithology classification

Kester D. Waters[1] and Michael A. C. Kemper[1]

Abstract

Full-stack seismic interpretation continues to be the primary means of subsurface interpretation. However, the underlying impact of amplitude variation with offset (AVO) is effectively ignored or overlooked during the full-stack interpretation process. Recent advances in well-logging and rock physics techniques highlight the fact that AVO is a useful tool not only for detection of fluid anomalies, but also for the detection and characterization of lithology. We evaluated an overview of some of the key steps in the rock physics assessment of well logs and seismic data, and highlight the potential to move toward a new convention of interpretation on so-called *lithology stacks*. Lithology stacks may come in a variety of forms but should form the focus of interpretation efforts in the early part of the exploration and appraisal cycle. Several case studies were used to highlight that subtle fluid effects can only be extracted from the seismic data after careful assessment of the lithology response. These case studies cover a wide geography and variable geology and demonstrate that the techniques we tested are transferable and applicable across many different oil and gas provinces. The use of lithology stacks has many benefits. It allows interpretation on a single stack rather than many different offset or angle stacks. A lithology stack provides a robust, objective framework for lithostratigraphic interpretation and can be calibrated to offset wells when available. They are conceptually simple, repeatable, and transferable, allowing close cooperation across the different subsurface disciplines.

Introduction

Many interpreters continue to use full-stack seismic sections in conventional seismic interpretation, focusing on establishing time and depth structure maps, which are subsequently used to identify structural (four-way, fault bounded, etc.) and stratigraphic (pinch outs, differential compaction, etc.) traps. An underlying assumption of this approach is that the stack amplitudes are responding to geologically meaningful boundaries, and that the denoising/signal boosting process of stacking over a range of offsets or angles provides the optimum data set for structural mapping. This assumption is also implicit in interpretation packages that offer automatic picking on a preselected event type such as a peak or trough or zero crossing. However, this assumption is often violated due to the amplitude variation with offset (AVO) inherent in the seismic data.

Stacked seismic sections can be thought of as the sum of the reflection coefficients over the stack range. These coefficients are dependent on the angle of incidence of the ray path from a given source-receiver pair and the elastic contrasts between the geologic layers causing the reflections, resulting in AVO. For many reservoirs, the presence of hydrocarbons can change the AVO behavior in such a way as to cause the seismic signature of the reservoir to change character on a stacked section. This change in behavior can often be useful as a hydrocarbon detection signal, as in the case of a simple (negative) event becoming brighter, which is often the case with class-3 AVO anomalies. In other cases, the changes are more subtle and less easy to interpret on full-stack seismic, such as a polarity reversal or a dim spot. In these latter circumstances the hydrocarbon bearing rocks can be completely missed.

In the past, understanding AVO has not been considered a requirement for structural interpretation. This is now changing. The significant uptake of AVO technology, particularly over the last 10 years, has resulted in more companies acquiring high quality compressional (P) and shear (S) sonic data. Analyses of these data have highlighted the fact that AVO can play an important role not only in the identification of fluids, but also in the identification of lithology. In addition, improvements in the understanding of rock physics and the availability of easy to use tools for modeling allows interpreters to anticipate the seismic character of potential reservoirs and ensures that the right seismic data sets are derived to optimally study potential reservoirs (in terms of geology and pore-fill).

[1]Ikon Science Ltd., London, UK. E-mail: kwaters@ikonscience.com; mkemper@ikonscience.com.

Manuscript received by the Editor 31 July 2013; revised manuscript received 10 December 2013; published online 20 March 2014. This paper appears in *Interpretation*, Vol. 2, No. 2 (May 2014); p. SC77–SC91, 11 FIGS.

http://dx.doi.org/10.1190/INT-2013-0118.1.

In this paper, we introduce the concept of "find the rocks, and the fluids will follow." In other words, we propose that interpreters should move away from conventional interpretation using full-stack data (or even partial-stack data, e.g., nears/fars) and instead initially produce and use the seismic product, which optimally brings lithological changes to the fore (litho stack). Then in a second phase, determine and use the seismic product, which optimally brings the effect of pore-fill to the fore (fluid stack). This approach, based on rock property modeling and AVO techniques, has proven successful on many projects.

The proposed method relies on the assumption that the seismic data can be manipulated to produce a result that is largely independent of the fluids. This is not always going to be possible and a clear understanding of the rock physics is required to assess this potential. In addition, the seismic data need to be of a quality that will permit such a manipulation. This paper starts by reviewing a typical rock physics workflow that will yield an understanding of the AVO characteristics of the rocks and fluids such that an appropriate manipulation of the seismic gathers may be possible. Subsequently, a review of the seismic data quality requirements and various AVO techniques is made. Thereafter, several case studies are presented followed by a discussion and conclusions.

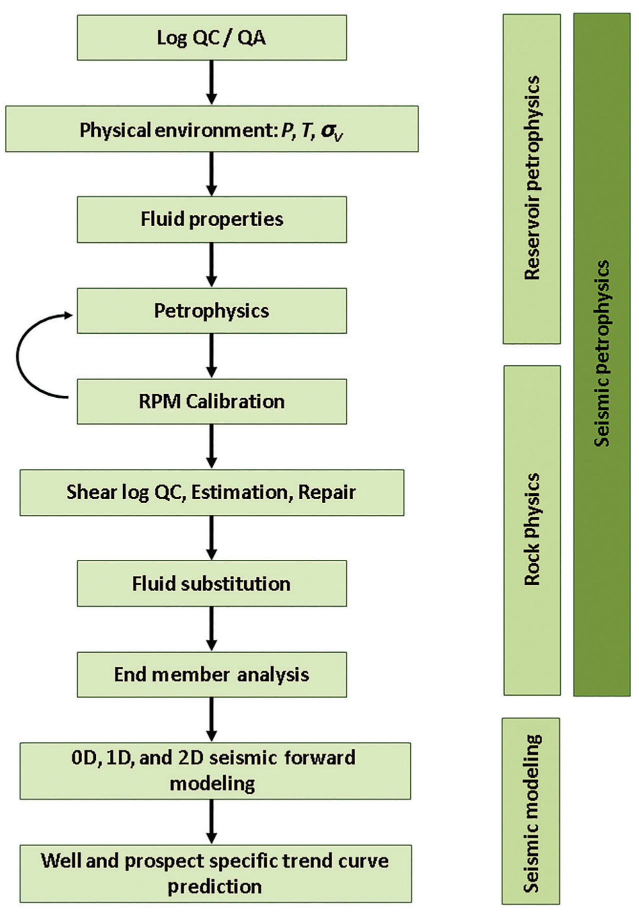

Figure 1. Overview of a rock physics, AVO, and inversion feasibility workflow. Note that rock physics model (RPM) calibration is a significant step in this workflow and can be used with good effect to QC and constrain the petrophysical interpretation.

Rock physics

Seismic interpretation requires a wide range of skill sets and considerable investment of time, as well as attention to detail. As such, it represents a significant time and cost element in the overall exploration and production cycle. Significant sums of money are spent on sophisticated interpretation packages, designed to improve and speed up the visualization and interpretation of subsurface data. But all this technology and know-how is at risk of being wasted if the interpreter has not done some groundwork to understand the basic relationships between the rock properties and seismic amplitudes, and has not processed the available seismic data to optimally emphasize the target reservoirs (and pore-fill). One might argue that such an understanding comes from the well-tie process (something that should be performed routinely before any interpretation). However, lateral facies changes, changes in pressure regime, etc. can all give rise to seismic responses that are quite different to those encountered at well control points.

Prior to commencing a seismic interpretation project it is critical that the interpreter creates a range of fit-for-purpose models for a range of potential scenarios. The seismic response for these models should be synthesized such that the expression of lithology changes and pore-fill, pressure changes, etc. can be understood. This is often referred to as a rock physics, AVO, and inversion feasibility study. An overview of the key steps in this type of study is outlined in Figure 1.

As log data forms the calibration, the first and very important step is that of log quality control. Here, we present a particular emphasis on the elastic logs: P-sonic, S-sonic, and density because their quality and availability will determine much of the subsequent seismic workflows. However, care should be taken to ensure that all log and core data are internally consistent. Care should be taken to identify and account for the effects of environmental problems (borehole caving and rugosity) and its impact on the various logging tools, e.g., cycle skipping in sonic data and mud readings on density logs. Additionally, the presence and impact of drilling mud invasion should be carefully reviewed and invasion profiles determined for use in the rock physics workflow.

The reservoir and, equally important, nonreservoir should then be assessed in terms of the physical environmental conditions, especially pressure (P), temperature (T), and vertical effective stress (VES). Downhole pressures are collected using a variety of tools, such as repeat formation tests, modular formation dynamics tests, and formation interval test tools, while temperatures come from the individual logging run bottom hole temperatures, after correction for mud circulation times. VES is typically derived by subtraction of the pore pressure (measured directly in the reservoir) from the overburden pressure (typically estimated by integration of the density log plus the static water column, if offshore). The density log should first be quality controlled using simple velocity-density transforms such as those proposed by Gardner et al. (1974). Using these site-specific P- and T-conditions, a suite of associated fluid acoustic properties can be determined using published models such as Batzle and Wang (1992) formulations or more recent models published by the Fluid and DHI consortium of Colorado School of Mines and University of Houston (known as *fluid application geophysics* and initiated by Han and Batzle, 2000). Typical inputs required for conventional fluids would be the formation water salinity, oil gravity using the American Petroleum Institute (API) definition, gas to oil ratio, associated gas gravity, and free gas gravity. For heavy oils, knowledge of the tool logging frequency might also be required. Some companies keep regional rock property databases that can be mined for analogues and appropriate values when data are not available at specific well locations (Waters, 2012). Typically, the interpreter might specify ranges of oil and gas properties to understand the sensitivity of key parameters and their impact on the fluid moduli. The final selection of parameters will have a direct impact on the estimated stiffness of the rock frame during Gassmann modeling, so care should be taken at this stage to avoid spurious fluid effects.

Petrophysical evaluation is subsequently performed to estimate clay volume fraction (along with other minerals), total and effective porosity, and total and effective saturation. Where appropriate, special analytical techniques (such as the method proposed by Thomas-Stieber, 1975) should be adopted to account for differences in clay and porosity systems and tool resolution (structural, laminated, and dispersed clay systems may have markedly different rock property behaviors). The process of petrophysical interpretation is too large a subject to discuss in detail in this paper; however, one clear statement that should be made is that petrophysical evaluation can and should be informed by rock physics diagnostics, and vice versa. The reader is referred to the article by Sams and Focht (2013) for an example of petrophysical interpretation constrained by rock physics. Where available, a thorough analysis of thin sections, X-ray diffraction, core data etc. should support the petrophysical interpretation such that the interpreter is aware of the geologic environment and depositional and diagenetic history (crucial for determining the right RPM).

In addition to compressional velocity (V_P) and density (ρ) profiles (both routinely acquired in wells), S-wave velocity data (V_S) is of pivotal importance to the success of any rock physics study. All three profiles are required for the computation of the bulk and shear moduli of the rock. Once these quantities are defined, there are a wide variety of different workflows/disciplines in which they may be used. In this paper, we will discuss their role in the seismic interpretation process. However, they also play a key role in e.g., pore-pressure analysis, geomechanics, and prestack seismic inversion, etc. It is the combination of contrasts in compressional, shear, and density data that control the AVO behavior of the rocks, even when only compressional wave seismic data are acquired. Therefore, gathering and properly quality controlling the V_S profile for deriving predictive models is a process of utmost importance.

S-wave data are typically quality controlled by comparison to existing models such as Greenberg and Castagna's (1992) published end member trends, and also by comparison to theoretical (e.g., Hashin and Shtrikman, 1963; Kuster and Toksoz, 1974) or heuristic/hybrid models (e.g., Wyllie et al., 1956; Wyllie, 1963; Avseth et al., 2000, 2005). Particular care should be taken when evaluating older logging tools where monopole instruments often failed. Also, particularly in slow or unconsolidated rocks, spurious readings often resulted. RPM overlays, showing contours of constant V_P/V_S ratio, for example, should always be used and care should be taken if extrapolating models beyond the limits of observed and recorded data. A good first-pass QC is to generate a Poisson ratio curve, which will immediately highlight problems arising due to inconsistency in V_P and/or V_S measurements, data misalignment or poor quality data. Log readings with Poisson ratio less than approximately 0.06 (the Poisson's ratio of pure quartz) or higher than 0.5 (physical upper limit) should be inspected in detail to determine the root cause of the issue and should either be rectified or be discarded. Once calibrated to good quality data, a RPM can be used to repair, extend, and predict shear curves (e.g., in wells where no shear sonic was logged). These data will later allow site-specific AVO models to be generated and reviewed and variations between sites to be assessed.

Once all of the data are gathered, fluid properties computed, mineral moduli determined, petrophysical analyses completed and logs repaired, the typical next stage in the rock physics workflow is to perform fluid replacement modeling. The most common approach is that of Gassmann (1951); however, other techniques can be considered, particularly where Gassmann's assumptions do not hold, such as in tight reservoirs, shales, etc. There are many textbooks (e.g., Mavko et al., 1998) where the Gassmann equations are presented, but we will not repeat them here. We will, however, present some best practices in Gassmann fluid substitution, as there are some pitfalls that should be avoided. In general, the interpreter should always first strip out the effect of fluids by substituting to the dry state. This so-called *dry rock QC* (an intermediate step in Gassmann) is crucial to ensure that geologically and physically plausible data are derived. For example, the interpreter should first confirm that dry rock Poisson's ratio falls within an expected physical range. In the first instance this means that dry rock Poisson's ratio does not show negative values, or values in excess of 0.5. For high porosity, unconsolidated rocks, or for slightly cemented rocks at very low effective stress, one might expect dry Poisson's ratio approximately 0.3–0.35. With increasing compaction (porosity reduction), consolidation, and/or cementation, one might expect dry rock Poisson's ratios of approximately 0.2 (or perhaps slightly less for highly cemented quartz rich sandstones). Another important QC is to look at consistency in dry rock Poisson's ratio between wells. Assuming that data lie within sensible bounds and show little scatter, the next step is to resaturate the data with the new pore fluid. However, should there be inconsistencies in the data, perhaps due to variability in log quality from one location to the next, or perhaps due to dispersed or laminated clay in the reservoir, the interpreter should consider imposing an appropriate dry rock model to constrain the Gassmann fluid substitution process. This process is outlined in the work presented by Simm (2007). After dry rock QC and modeling, fluid replacement to the new fluid (changed fluid properties and/or saturation) can take place with improved confidence. See Figure 2 for examples of dry rock QC plots for a variety of scenarios.

The upper left plot shows the dry rock behavior of an Eocene, relatively shallow, unconsolidated oil and gas bearing sandstone reservoir (after fluid substitution to dry). These dry rock QC plots allow the interpreter to assess the dry pore space stiffness of the rocks in question and to quickly evaluate their fluid sensitivity. Dry pore space stiffness can be considered as the contribution of the pore space to the total porous rock compressibility (i.e., the porous rock compressibility is equal to the mineral compressibility plus pore space compressibility; Mavko, 1998). Upper and lower bounds, interpolated along the lines of constant pore stiffness can be used to constrain the Gassmann fluid substitution effect. In this instance, large fluid effects would be anticipated based on the wide spacing of the pore-stiffness lines (a proxy for fluid substitution magnitude). The upper right plot shows an example of the Fulmar reservoir of Jurassic age, which is considerably deeper (approximately 18,000 ft), well consolidated, and at a very high temperature and pressure. In this example, we apply a dry rock model based on the constant cement model (Avseth, 2000) for clean quartz rich sandstone. When applying the dry rock model, the starting dry rock input into Gassmann's equations, which are used to compute the fluid effect, is taken from the model rather than the measured data points (Simm, 2007). The computed difference (i.e., bulk modulus from initial to final fluid conditions) is then applied back to the original data. This process of applying the initial to final difference based on a model, imposes a systematic fluid effect for a given porosity and shale content. It is therefore a useful methodology in cases in which, e.g., dispersed or laminated clays cause problematic dry rock behavior, or where a systematic fluid effect is desired across several wells where data quality is variable (e.g., shear logs in unconsolidated environments often present log quality issues: This methodology ensures that unreasonable, i.e., overly large fluid effects, are not produced through Gassmann fluid substitution).

The middle row of Figure 2 shows an example of oil-based mud (OBM) invasion into a brine-bearing formation. The left plot shows the computed dry rock properties assuming in situ brine-bearing conditions, which give rise to very low and negative values of $K_{\mathrm{dry}}/K_{\mathrm{min}}$ (normalized bulk modulus). After correcting the input saturation curve, allowing for the presence of OBM in the pore space, we find an improved dry rock behavior, in line with the response observed in other reservoirs under similar pressure and temperature conditions. In this example, V_{P}, V_{S}, and Rhob logs all need correcting for invasion.

The bottom row of Figure 2 shows an example of water-based mud (WBM) invasion into a gas-bearing reservoir. In this case, we have control data in the water leg of the sandstone reservoir and are able to compare the response above and below the contact. Inspection of the dry rock plot on the left shows two clusters of data points. By coloring the dry rock data by the in situ saturation, it becomes clear that the upper cluster of data correspond to where gas has been interpreted from the log (resistivity) data. Computation of the invasion saturation profile (SXOE) using the micro or shallow resistivity log provides an alternative scenario to explore, shown on the right plot. After allowing for WBM invasion, we now observe a consistent dry rock behavior across the gas/water contact — a far more geologically plausible scenario. In this example, V_{P}, V_{S}, and Rhob logs again all need correcting for invasion.

When applying Gassmann's fluid substitution to log data, these dry rock QC plots become a useful tool not only to identify and confirm geologic characteristics of reservoirs, but also to understand and investigate uncertainties in the underlying petrophysical interpretations. Some examples are outlined below.

OBM invasion into a brine-bearing reservoir: Ignoring OBM invasion and assuming brine-bearing conditions during Gassmann substitution will result in a softer (i.e., lower pore stiffness) than expected signature and potentially lead to an overestimation of the fluid effect.

WBM invasion into a hydrocarbon-bearing reservoir: Ignoring WBM invasion and assuming in situ hydrocarbon saturations during Gassmann substitution will result in a stiffer (i.e., higher pore stiffness) than expected signature and potentially lead to an underestimation of the fluid effect.

Low or residual saturation gas can have a dramatic effect on the calculated properties of the dry rock frame. It is crucial, therefore, to understand whether low saturations are genuine, or a result of petrophysical misinterpretation. Incorrect assumption of low gas saturation, perhaps as low as just a couple of percent, is compensated by interpreting a significantly stiffer than expected rock frame, resulting in much reduced fluid sensitivity.

Over estimation of the shale (effective porosity system) or clay (total porosity system) mineral moduli will result in a softer rock (where reservoirs have a

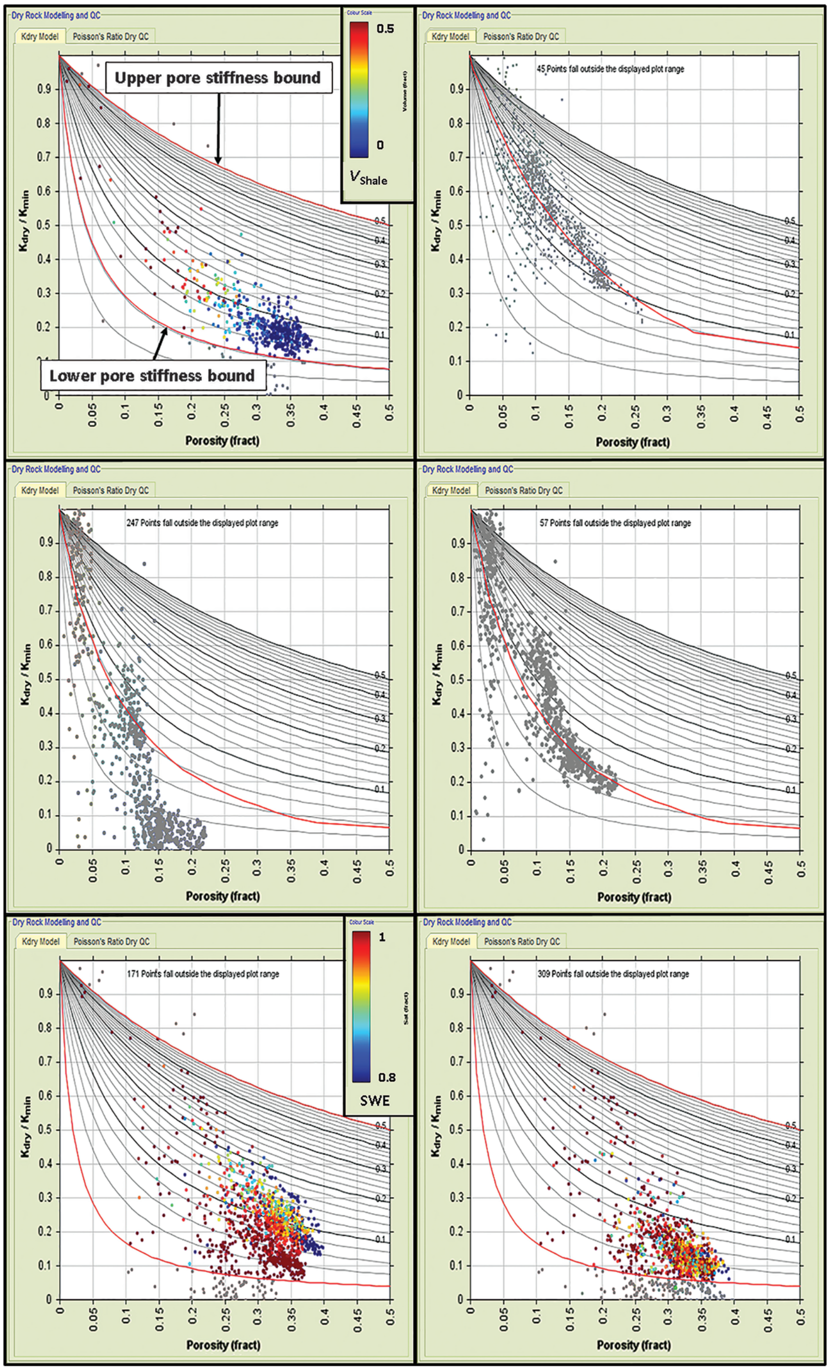

Figure 2. Six examples of dry rock QC and modeling plots from a Central North Sea study. The plots show the normalized dry bulk modulus (dry bulk modulus K_{dry} divided by mineral bulk modulus K_{min}) versus porosity for a range of examples. The upper left plot shows the dry rock behavior of an Eocene, relatively shallow, unconsolidated oil and gas bearing sandstone reservoir. Upper and lower bounds (shown in red), interpolated along the lines of constant pore stiffness can be used to constrain the Gassmann fluid substitution effect. In this instance, large fluid effects would be anticipated based on the wide spacing of the pore-stiffness lines (a proxy for fluid substitution magnitude). The upper right plot shows an example of a Jurassic, Fulmar aged reservoir, which is considerably deeper (approximately 18,000 ft), well consolidated, but at a very high temperature and pressure. In this example, we apply a dry rock model based on the constant cement model for clean quartz rich sandstone. In this instance, the magnitude of the fluid effect is computed from the model and applied to each of the data points. This becomes a useful methodology where dispersed or laminated clays cause problematic dry rock behavior, or where a systematic fluid effect is desired across several wells where data quality is variable. The middle row shows an example of OBM invasion into a brine-bearing formation. The left plot shows the computed dry rock properties assuming in situ brine-bearing conditions, which give rise to very low and negative values of $K_{\mathrm{dry}}/K_{\mathrm{min}}$ (normalized bulk modulus). After correcting the input saturation curve, allowing for the presence of OBM in the pore space, we find an improved dry rock behavior, inline with the response observed in other reservoirs under similar pressure and temperature conditions. In this example, V_{P}, V_{S}, and Rhob logs all need correcting for invasion. The bottom row shows an example of WBM invasion into a gas-bearing reservoir. In this case, we have control data in the brine leg of the sandstone reservoir and are able to compare the response above and below the contact. Inspection of the dry rock plot on the left shows two clusters of data points. By coloring the dry rock data by the in situ saturation, it becomes clear that the upper cluster of data correspond to where gas has been interpreted from the log (resistivity) data. Computation of the invasion saturation (SXOE) using the micro or shallow resistivity log provides an alternative scenario to explore, shown on the right plot. After allowing for WBM invasion, we now observe a consistent dry rock behavior across the contact — a far more geologically plausible scenario. In this example, V_{P}, V_{S}, and Rhob logs all need correcting for invasion.

significant shale/clay fraction). The reverse is true for their underestimation.

Over or underestimation of the petrophysical clay or shale volume fraction can impact the pore stiffness considerably. It is highly recommended to ensure consistency in the petrophysical interpretation when working across multiple wells.

Once a variety of fluid saturation cases have been generated (e.g., low [residual] and high saturation gas or various hydrocarbon column thicknesses) the next step is to generate corresponding AVO synthetic gathers, impedance, and other rock property log curves. Profiles such as acoustic impedance (AI), gradient impedance (GI), elastic impedance (EI), extended elastic impedance (EEI), V_P/V_S ratio, Poisson's ratio, Lambda-Rho, Mu-Rho etc., can be derived from the V_P, V_S, and Rhob data measured in the well and conditioned appropriately (as described above). Once derived, they should be analyzed, within the context of geologic, petrophysical, and seismic facies in the wells. Relationships between facies, petrophysical properties, and their corresponding elastic (e.g., AI/$V_P V_S$ or AI/GI) response (at their corresponding scales) should be assessed.

It is important to distinguish between the different uses of the term *facies*. To the geologist, facies descriptions typically exist at the cm-m scale, and consist of detailed descriptions of rocks (typically from core) and logs and a corresponding interpretation of depositional environment and underlying geologic process. The petrophysicist may further define electrofacies, whereby the core data are analyzed alongside the logged response and may be used to perform a supervised classification (often using many input training curves) of logs in wells that lack core facies control. For the purpose of seismic analysis and inversion feasibility, it is important to understand to what degree these facies are separable in the elastic domain at log and seismic scale. For example, a 20-m-thick sandstone, consisting of 10 or more geologic facies may represent perhaps only two different elastic facies, relating perhaps to changing clay content. Hence, we reduce 10 geologic facies into just two corresponding log-scale elastic facies. Once these underlying log data are reviewed at the seismic scale, it may be that the differences in elastic properties of the two log-scale elastic facies collapse, such that only a single seismic facies needs be defined, because the process of seismic inversion would be unlikely to resolve more facies.

In general, for the purpose of inversion feasibility, it is therefore useful to classify log responses by their elastic facies (guided by the petrophysical interpretation).

Once the log-scale analysis has been performed, it is common practice to upscale the data to the seismic domain (by application of filters) to reassess the robustness of the relationships at seismic scale. It is useful to consider band-limited inversion as well as absolute inversion at this stage — particularly in geologically complex areas where construction of a robust low-frequency model might be problematic. Figure 3 shows a typical well-log display that might be generated and reviewed prior to conducting a seismic interpretation (of either reflectivity or impedance data). In this example, we show results of a fluid substitution process in a North Sea well. Tracks a-e show the log-scale results, where a is the V_{shale} interpretation, b is the derived elastic facies, c is the interpreted porosity, and d and e are the AI, and V_P/V_S ratio for brine (blue) and oil (green) bearing cases. Tracks f-i show the same AI and V_P/V_S profiles after upscaling to the seismic bandwidth. Here, the low frequencies are retained, and hence, these results would be useful for determining the applicability of, e.g., simultaneous inversion (or any model-based inversion where low-frequency information is provided by the interpreter). Importantly, the facies log must be recomputed from the upscaled petrophysical data, because facies boundaries and layers will reorganize themselves depending on the bandwidth and resolving power. In this instance, f is the upscaled V_{shale} interpretation, g is the upscaled facies, h and i are the upscaled AI and V_P/V_S ratio for brine (blue) and oil (green) bearing cases. Lastly, tracks j-n show the relative (band-limited) profiles. Track j shows the band-limited V_{shale} log. Tracks k and l show the band-limited AI and V_P/V_S. Tracks m and n show the lithology and fluid relative impedance traces, generated from targeted EEI angles. Green fill indicates the fluid effect after fluid substitution from brine to oil. In this case, the lithology impedance (m) correlates closely with the band-limited V_P/V_S. The fluid impedance (n) shows a strong fluid effect, with near-zero values for the brine case and strong negative values for the oil case.

AVO techniques and seismic data conditioning

There is a wide variety of AVO techniques used across the oil and gas industry. Depending on the region you work in, the company you work for and the people you work with it, is very likely there is a preferred processing flow and a routine approach. It is worth noting that all of the different AVO techniques are all inherently linked. The first step, however, should be to decide whether you need an AVO reflectivity analysis or an AVO inversion to impedances (based on rock physics workflow and assessment of the seismic data quality/noise content, available angle ranges, etc.).

There are a handful of particularly useful techniques for derivation of lithology (and fluid) sensitive volumes. Below, we discuss a few of the more commonly used AVO techniques for deriving such volumes.

Intercept and gradient using Aki and Richards (1980) approach is one of the most commonly used techniques in AVO work. The intercept and gradient volumes are used to classify the seismic response into the different AVO classes. While useful, the two resulting volumes from this technique can often be difficult to interpret and full of ambiguity. An even simpler approach is to multiply the intercept and gradient volumes. When this is done, class-3 AVO anomalies are readily highlighted as large positive signatures. However, other more subtle AVO classes can easily be missed. Simpler, still is to only use the gradient volume. This volume, which is sensitive to changes in Poisson ratio, can be a good lithology indicator. However, it can often be very noisy, and therefore requires careful processing (everything up to and including migration) and seismic conditioning (postmigration) to make it suitable for interpretation.

The AVO formulations of Smith and Gidlow (1987) and Fatti et al. (1994) allow multiple angle stacks to be transformed simultaneously to P-wave reflectivity (R_{p}), S-wave reflectivity (R_{s}), and density reflectivity (R_{rho}). The most widely adopted technique is to then perform a weighted stack of the R_{p} and R_{s} volumes to provide what is widely referred to as fluid factor. Note that the S-wave reflectivity by its very nature is often a good lithology indicator (because most rocks show large differences in rigidity). Again, these products can be inverted individually in a variety of different ways to their corresponding impedances.

The EI technique (Connolly, 1999) provides an AI equivalent for nonzero-offset reflectivity data. This allows the direct inversion of, e.g., far-offset (angle) stacks to EI volumes that can be calibrated at well control points. A common approach is to color invert (Lancaster and Whitcombe, 2000) or perform sparse spike inversion of the single angle stack. A key benefit of this approach is that it avoids the complexities of combining multiple angle stacks (which may have differences in frequency content, phase, and alignment) and is therefore particularly robust.

The extended EI technique tunes the seismic inversion product (by rotation or weighted stacking of AI and GI inversions) to particular petrophysical properties (Whitcombe, 2002; Connolly, 2010). The same methodology can be applied directly to AVO intercept (I) and gradient (G) volumes. The general workflow is to define, from well data, those rotation or chi angles that are most sensitive (or insensitive!) to, e.g., V_{clay}, or S_w and

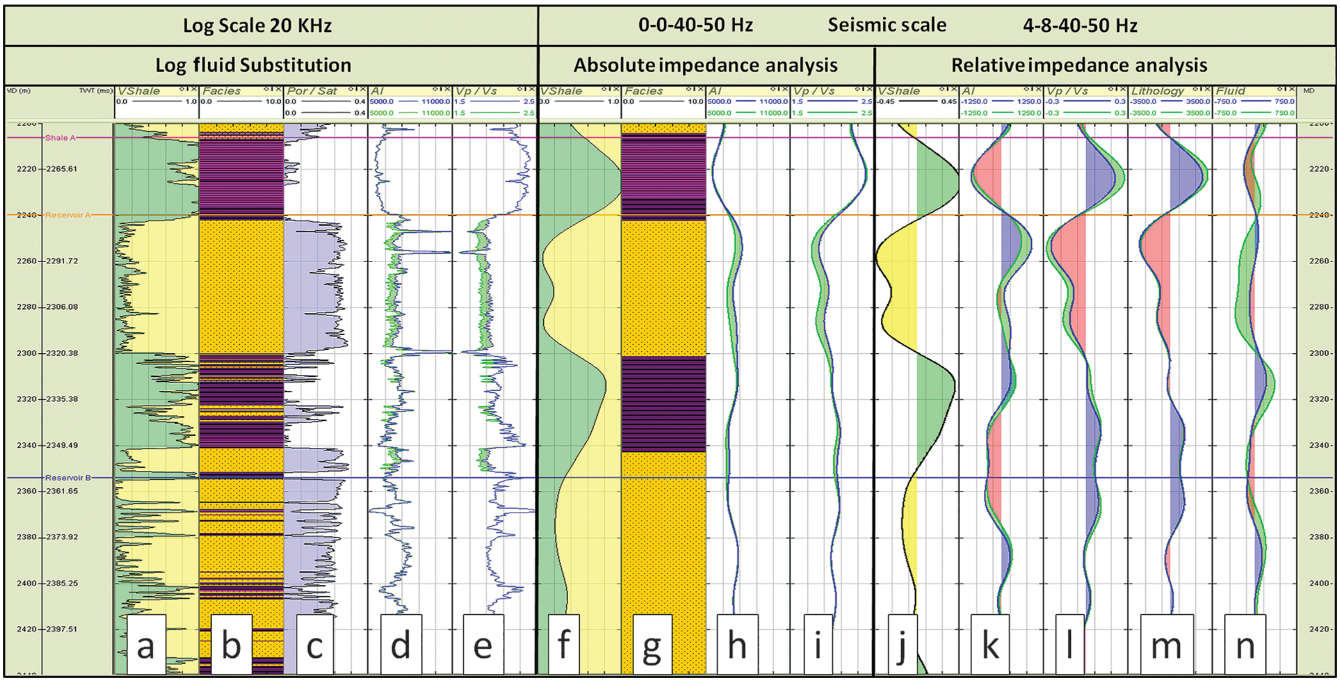

Figure 3. Example of well log feasibility study. This plot shows a typical well log display that might be generated and reviewed prior to conducting a seismic interpretation (of either reflectivity or impedance data). In this example, we show results of a simple fluid substitution process in a North Sea well (the modeling in this well corresponds to the case study shown in Figure 7). Tracks a-e show the log-scale results, where a is the V_{shale} interpretation, b is the derived facies, c is the interpreted porosity and d and e are the AI, and $V_{\mathrm{P}}/V_{\mathrm{S}}$ ratio for brine (blue) and oil (green) bearing cases. Tracks f-i show the AI and $V_{\mathrm{P}}/V_{\mathrm{S}}$ data after upscaling to the seismic bandwidth. Here, the low frequencies are retained, and hence, these results would be useful for determining the applicability of, e.g., simultaneous inversion (or any model-based inversion where low-frequency information is provided by the interpreter). Importantly, the facies log must be recomputed from the upscaled petrophysical data. In this instance, f is the upscaled V_{shale} interpretation, g is the upscaled facies, h and i are the upscaled AI and $V_{\mathrm{P}}/V_{\mathrm{S}}$ ratio for brine (blue) and oil (green) bearing cases. Lastly, tracks j-n show the relative (band-limited) profiles. Track j shows the band-limited V_{shale} log. Tracks k and l show the band-limited AI and $V_{\mathrm{P}}/V_{\mathrm{S}}$. Tracks m and n show the lithology and fluid relative impedance traces, generated from targeted EEI chi angles. Green fill indicates the fluid effect after fluid substitution from brine to oil. In this case, the lithology impedance (m) correlates closely with the band-limited $V_{\mathrm{P}}/V_{\mathrm{S}}$. The fluid impedance ($n$) shows a strong fluid effect, with near-zero values for the brine case and strong negative values for the oil case.

then derive EEI reflectivity volumes (by combining I and G) or EEI impedance volumes (by combining AI and GI). This is often done in the first instance by cross-correlating EEI curves for a full range of chi angles to selected petrophysical curves. While useful, this process often shows that high correlations to certain petrophysical curves, such as V_{shale} or porosity occur at very similar angles, making it difficult to separate out different properties. In addition to this, the well data that are fed into this process can often be biased (e.g., with a majority of wells being hydrocarbon bearing) and can therefore give rise to results that are skewed (particularly important when correlating water saturation curves). Therefore, a second complementary approach, which uses a facies-based scheme is often more instructive, and directly relates log based facies to seismic properties. Figure 4 upper left shows a facies-based EEI analysis for the North Sea field shown in Figure 6. For each facies, the mean EEI is computed as a function of the chi angle. This allows the interpreter to determine how the chi angle reflection coefficient will change between different pairs of facies for different angles. The objective now becomes that of defining chi angles at which key facies cross over. In other words, where the impedance contrast between two facies is minimized, giving rise to zero reflectivity. There are two important angles to derive from this plot. First, the angle at which the brine and hydrocarbon sand facies intersect defines the lithology angle. At this angle, the fluid effect is minimized; however, it should be noted that because this is often a large negative angle, it can be particularly sensitive to porosity changes. Second, the angle at which the brine sand and shale facies intersect defines the fluid angle. At this angle, the lithological effect is minimized. Care should be taken to properly assess and define the petroelastic facies prior to this analysis as often there are changes in shale types (typically associated with changing depositional styles) above, in between and below the reservoirs of interest. Finally, there is a third aspect that should be investigated through crossplot analysis of lnAI and lnGI. This is the angle of rotation of the porosity trend, i.e., a regression along the brine-bearing sandstone trend. This chi angle is often referred to as a *lithofluid projection* or *porosity trend*. A rotation at this angle will give a product that is sensitive to facies and fluid changes, but relatively insensitive to porosity (unlike the lithology angle). EEI reflectivity or EEI impedance volumes at these three

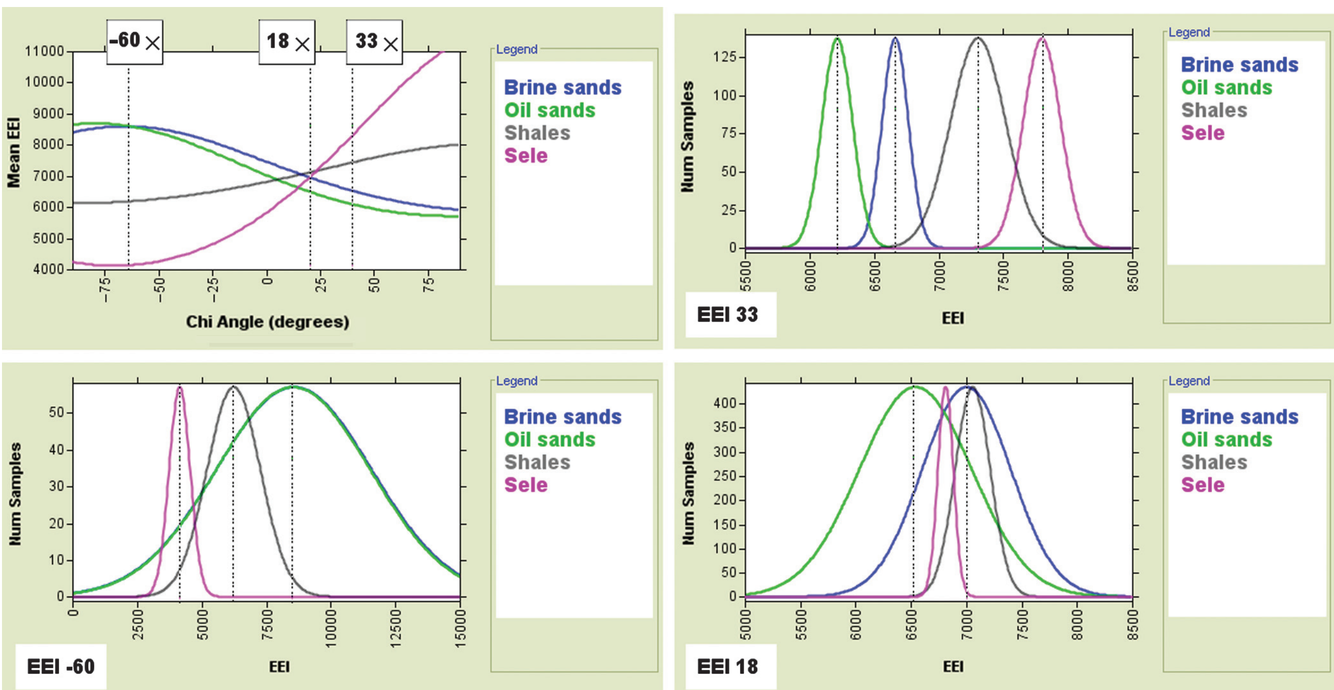

Figure 4. EEI facies-based feasibility analysis. The upper left plot shows a facies-based EEI analysis for the North Sea field shown in Figure 6. For each facies, the mean EEI is computed as a function of the chi angle. This allows the interpreter to determine how the chi angle reflection coefficient will change between different pairs of facies for different angles. The objective now becomes that of defining angles at which key facies cross over. In other words, where the impedance contrast between two facies is minimized, giving rise to zero reflectivity. There are two important angles to derive from this plot. First, the angle at which the brine and hydrocarbon sand facies intersect defines the lithology angle. At this angle, the fluid effect is minimized; however, it should be noted that because this is often a large negative angle, it can be particularly sensitive to porosity changes. Second, the angle at which the brine sand and shale facies intersect defines the fluid angle. At this angle, the lithological effect is minimized. Care should be taken to properly assess and define the petroelastic facies prior to this analysis as often there are changes in shale types (typically associated with changing depositional styles) above, in between and below the reservoirs of interest that will need to be investigated and understood.

rotation angles should be used in conjunction during the interpretation process. It is often preferable to derive EEI reflectivity volumes in the first instance, as it allows for additional reflectivity domain denoising and conditioning to be applied. Once the EEI reflectivity volumes are optimal, they can then be inverted individually to the corresponding EEI impedance volume using, e.g., colored, sparse spike, or deterministic inversion techniques. EEI is used extensively in the case studies below.

Before deriving these various AVO products, the interpreter should first perform a detailed QC of the prestack data. In the first instance, this should be performed by comparison of Zoeppritz (1919) synthetic gathers, to observed seismic responses at well locations.

Computation of root-mean-square (rms) amplitude maps of each stack in and around the interval of interest will highlight any imaging problems associated with e.g., shallow gas or fault shadows. Correction maps (i.e., scalar or weight maps) can later be derived (by normalization of the rms maps), which can either be directly applied to the seismic or be used to control interpolation between pairs of wavelets (i.e., wavelets derived inside and outside of the affected areas) during the inversion process. The interpreter should generate and compare the frequency spectra of each angle stack. For AVO analysis (i.e., for any of the above methods), it is important that all stacks have a similar bandwidth, so spectral equalization should be applied prior to computation of the AVO products.

Assess the phase of each angle stack. This is typically performed by estimating wavelets from each angle stack using techniques such as partial coherence matching (White, 1980). It is important that the phase of the angle stacks is constant across the angle range. For colored inversion, an underlying assumption is that the data are zero phase. If that is not the case, the data should be remedially zero phased.

Compare the trace alignment between pairs of angle stacks. In the first instance, this might be performed by overlaying a wiggle display of the far offsets on a color display of the near offsets. Be cautious in geologic environments where AVO is expected to cause a polarity flip in reflectors at intermediate incidence angles. In these cases, stack data may not be expected to appear flat across the angle range. This should be verified by full wavefield synthetics generated at the wells. A second useful QC is to compute the crosscorrelation and time shift between pairs of stacks (around the target interval), and to assess whether there are any systematic problems related to residual move out or shallow overburden effects.

Assess the scaling of the data. Most modern data sets use amplitude preserving processing flows; however, it is not unusual that scaling of the offset data needs to be applied. One practical workflow that one might adopt is that of Ross and Beale (1994), whereby the relative scaling of near and far synthetics are compared to the corresponding near and far seismic volumes, typically in a background window away from hydrocarbon bearing zones. Correction factors can be derived and subsequently applied to the seismic data before AVO products are computed.

The objective of the interpreter is to apply seismic data conditioning techniques to optimize the derived AVO products (and corresponding impedances) such that they can be reliably calibrated to well data and used to predict reservoir and fluid presence away from known control points.

A typical AVO postprocessing flow is outlined in Figure 5.

Case studies

We start this case study section with the Brenda Paleocene oil field, which is located in block 15/25 in the UK North Sea. The Brenda field, at a depth of approximately 2 km, consists of deep water turbidite channels and lobes of Paleocene age (Balmoral sandstones) encased in shales of the Sele and Lista formations, forming a stratigraphic trap. The Brenda accumulation was first drilled by Conoco with the 15/25b-3 well in 1990. The well, which targeted a four-way dip closure, encountered just 20 ft of pay and tested 2690 bbl/day of 39° API oil from the Forties sandstones. The well was subsequently abandoned and the discovery left undeveloped, presumably noncommercial. OilExco plc, a Canadian start-up entered the UK North Sea and reassessed the 15/25b-3 well and seismic data, using simple AVO modeling techniques. RPM showed that the combination of EI and GI (in this case the lithology volume) could be used to first discriminate sandstones from

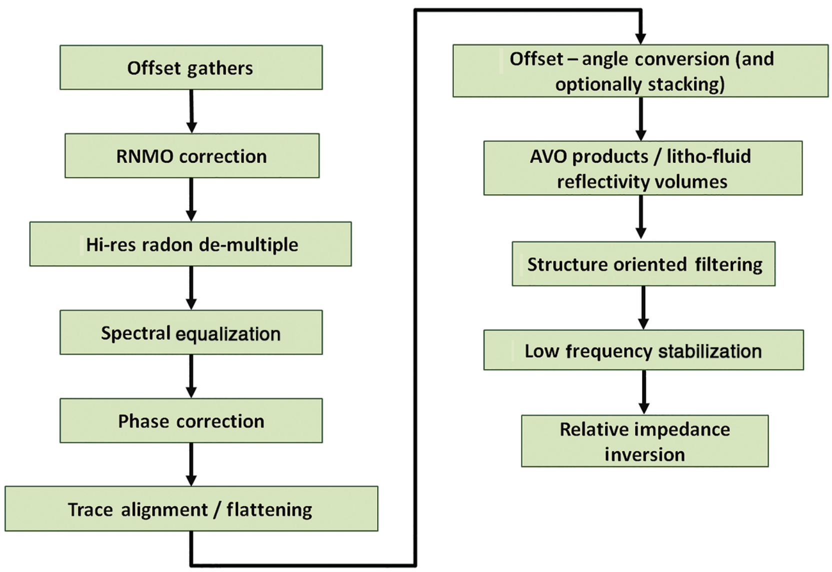

Figure 5. Workflow for postprocessing of seismic data for AVO analysis.

shales (using GI) and then to detect the oil-filled sandstones with high confidence (using EI). A new well was planned (15/25b-6), which targeted a structurally deeper and low-relief interpreted oil-filled sand channel. This was based on a low EI (far-offset colored inversion) anomaly, which was consistent with AVO modeling studies conducted at the nearby wells. The well encountered a series of oil-filled sandstones, the thickest of which was 26 ft and resulted in the announcement by Oilexco of the Brenda accumulation on 26th January 2004. The second well, targeting the second EI anomaly, encountered a 70-ft-thick sand and tested 40 API crude at a flow rate of 4785 bbl/day. Thirteen successful appraisal wells were then drilled in rapid succession, using the EI/GI approach, ultimately leading to first oil under three years later. This case study demonstrates that by understanding the attribute behavior through RPM before seismic interpretation, along with subsequent targeting of specific lithology and fluid sensitive seismic products, it is possible to extract a significantly more useful and interpretable geologic image from the subsurface (Jones et al., 2004).

The model in Figure 6 shows the colored inversion of a synthetic full-stack seismic section and corresponding lithology reflectivity generated by interpolating the well data shown in Figure 3. Random normal noise has been introduced into the underlying V_P, V_S, and Rhob models (using correlated Monte-Carlo simulations), which

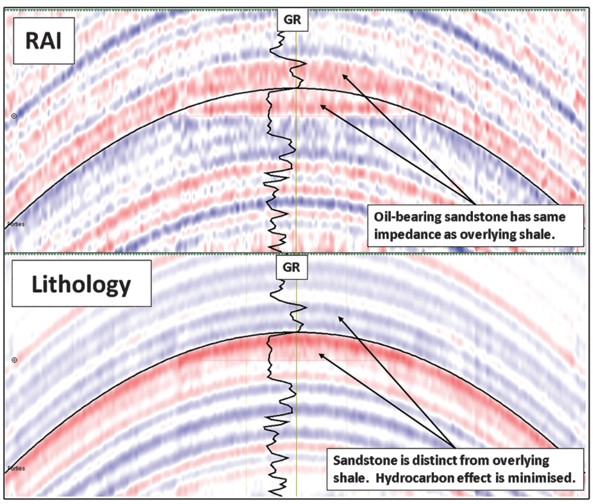

Figure 6. Example of simple model constructed using a well (gamma ray log displayed). The model was constructed using a normal SEG wavelet-processed polarity wavelet, where a downward increase in impedance produces a peak. Random normal noise has been introduced into the underlying V_P, V_S, and Rhob models (using correlated Monte-Carlo simulation) and used to construct synthetic near, far, and full-stack models. The lithology section in this instance was generated by rotation of intercept and gradient products (computed from near and far synthetics) to a lithology sensitive chi angle. The full stack and lithology stacks were then color inverted to provide relative acoustic impedance (RAI) and relative lithology impedance products.

were used to construct the starting synthetic models. A hydrocarbon contact was subsequently inserted into the model at the top of the anticline feature and fluid substitution was performed to an oil-bearing state above the oil-water contact, to simulate a real world scenario. The lithology section in this instance was generated by rotation of intercept and gradient products (computed from near and far synthetics) to a lithology sensitive chi angle, determined from extended EI analysis of the log data. The implication of this modeling exercise is that hydrocarbon-filled structural and stratigraphic traps will potentially be missed when using full-stack data because reservoirs under these conditions have the same impedance as the overburden shales. The lithology volume minimizes fluid effects and emphasizes the sand to shale contrasts.

Figure 7 shows average impedance map extractions from three relative impedance inversions over a Paleocene North Sea field. The average impedance extractions were performed in a short window below the top reservoir. The data are SEG wavelet-processed polarity, in which a positive peak represents an increase in impedance. Red and orange colors therefore represent soft events in the seismic. The green outline on the maps shows the approximate closing structural contour. The AI data are responding to a mixture of lithological and fluid variability in the subsurface — The fluid response is there, but where? The lithology volume highlights a significant channel complex and associated fan lobes, which cannot be identified from the AI data. The lower image shows the corresponding fluid impedance volume extraction. It would be true to say that only once the sand fairways have been delineated using the lithology extraction shown in the middle image, can be a confident interpretation of the fluid effects be shown in the lower image. Using these two volumes in conjunction allows for accurate prediction of reservoir presence, quality, and fluid fill.

In Figure 8, the displayed dip section through the derived lithology volume highlights channel and fan geometries, which are otherwise very difficult to determine from the homogenous and almost layer-cake appearance of the AI data. This is confirmed by detailed analysis of corresponding horizon slices through this interval (not presented in this paper). The data are again SEG wavelet-processed polarity. In these displays, black represents an acoustically hard layer. In this case, we observe that low angle-dipping reflectors in the AI data between the blue and pink horizons do not necessarily correlate to lithological boundaries identified by the lithology volume. In a manner similar to conventional prospecting and high grading (source, seal, migration etc.), it is important that the interpreter first defines a valid trap (stratigraphic, structural etc.), followed by determination of reservoir presence and quality and ultimately then determines the presence of hydrocarbons. These three risk elements can be interpreted by, for example the inspection of the three chi angle volumes described earlier, which are sensitive to reservoir (and fluid) presence (i.e., porosity angle), reservoir quality (i.e., lithology angle), and lastly fluid presence (i.e., fluid angle). A key aspect of the lithology volume is that it brings the major lithofacies changes to the fore, allowing the interpreter to quickly focus on viable reservoir targets.

In Figure 9, we show an example from a North Sea Eocene field where sandstones are unconsolidated and show strong fluid effects. Contrary to the seismic of the Brenda case study, the seismic here is SEG reverse polarity. Black events are therefore soft in the upper seismic display. In this example, the reservoir that is a hard reflection when wet, becomes a dim reflection when oil bearing and a soft reflection when gas bearing. Interpreting the various fluid contacts using full or angle stack reflectivity data alone could be a very subjective task. The lower image shows a lithology volume (MuRho) generated from a simultaneous inversion. Blue colors denote shale lithology, while hot colors denote sandstone presence. Note that MuRho is the square of the shear impedance, so shear reflectivity (Rs) generated from inversion of the reflectivity data using Fatti's formulation would work equally well and provide a lithology stack. Interpretation of the sandstone bodies and geometries is simplified because the fluid effects have been suppressed. The interpreted red horizon, made on the lithology volume provides an objective way of picking across the gas contact, where a seismic polarity reversal is observed. Images are taken from Min-Hoe et al. (2008).

Figure 10 shows a North Sea example of a Paleocene reservoir. The data are again SEG reverse polarity. Black colors represent soft lithologies. The interpretation of the green horizon on the upper image, RAI, would not be possible using a conventional full-stack impedance volume. The lithology volume (EEI in this example) in the lower image provides a clearer image of the reservoir, regardless of fluid fill. In this case, the response is consistent with hydrocarbon-bearing reservoir and confirmed with offset well data where an identical response is encountered.

Figure 11 shows a West Africa example. Data are SEG wavelet-processed normal polarity. Blue colors

a)
b)
c)
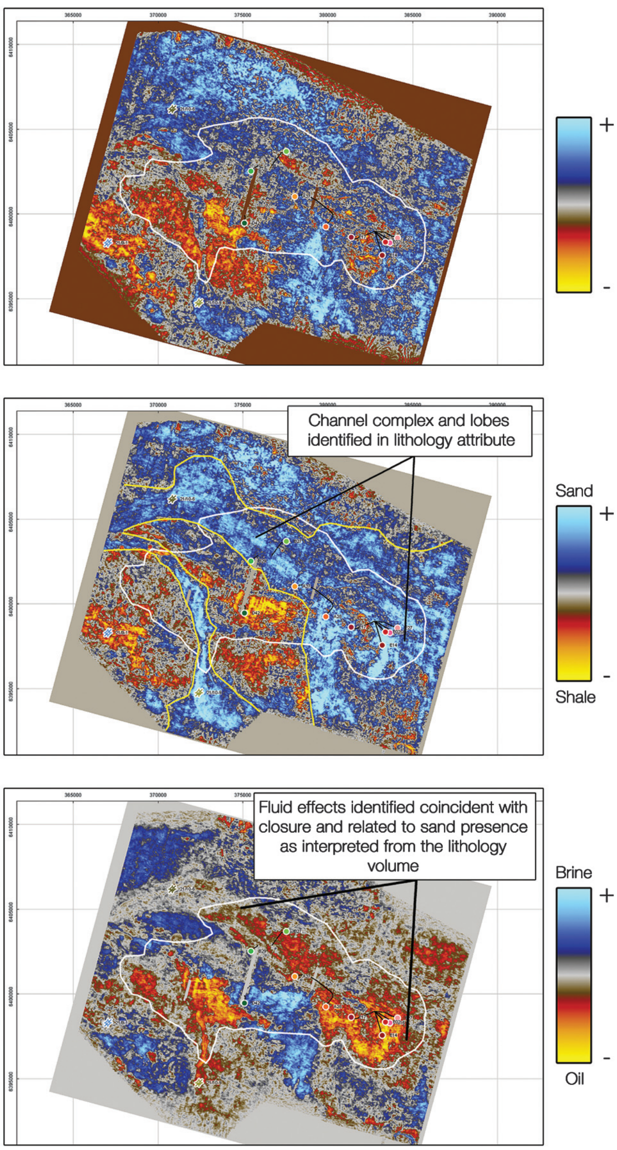

Figure 7. Average relative AI (a) and corresponding lithology impedance (b) extracted in a window below top reservoir over a Paleocene North Sea field and (c) shows the corresponding fluid volume, which shows polarity reversal (orange colors) coincident with the structural spill point (green outline).

a)
b)
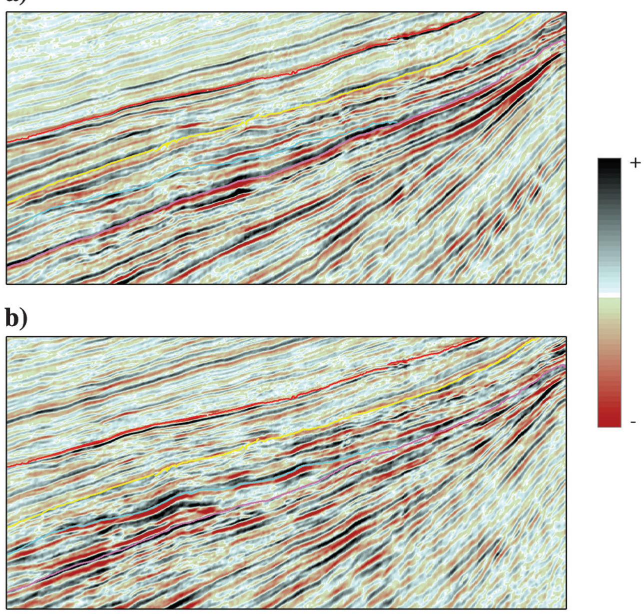

Figure 8. Relative AI (a) and corresponding lithology impedance (b) over a Cretaceous stratigraphic prospect in West Africa. Data are SEG wavelet-processed polarity, where a peak is a hard, downward increase in impedance. In these displays, black represents an acoustically hard layer. In this case, we observe that low angle-dipping reflectors in the AI data between the blue and pink horizons do not necessarily correlate to lithological boundaries identified by the lithology volume.

therefore represent hard layers. A meandering channel complex is clearly illuminated by the lithology volume between the blue and green horizons. This response is characteristic of highly sinuous channels in deep water environments and has been confirmed by detailed seismic mapping and attribute extraction. The benefit of the lithology volume in this case is that it helps to suppress high reflectivity/impedance events that are not related to reservoir presence. This allows for a more focused interpretation effort. In this case, it would be difficult (if not impossible) to map the reservoirs using AI because, as is shown by comparison of the lithology and AI data (see solid lines), the reservoirs appear as hard and soft AI layers.

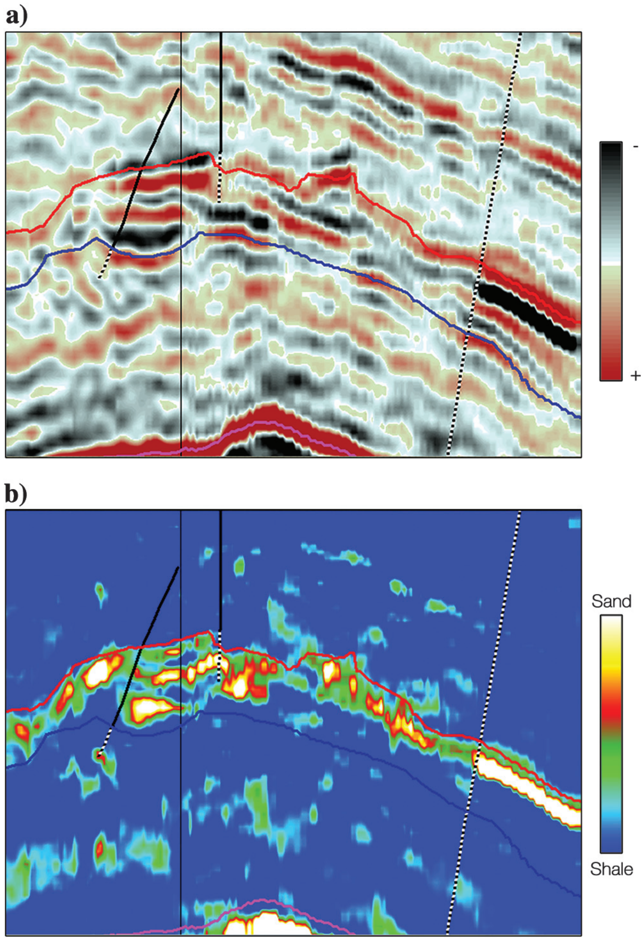

Figure 9. Full-stack reflectivity and corresponding lithology volume derived from a simultaneous inversion of data over an Eocene North Sea field. Data are SEG wavelet-processed reverse polarity, where a downward increase in impedance is a trough or negative number. Black events are therefore soft in the upper seismic display. In this example, the reservoir that is a hard reflection when wet, becomes a dim reflection when oil bearing and undergoes a polarity reversal when gas bearing. Picking across the various fluid contacts using reflectivity data alone could be a very subjective task. The lower image shows a lithology volume (MuRho) generated from a simultaneous inversion. Interpretation of the sandstone bodies and geometries is simplified because the fluid effects have been suppressed.

Discussion

In this paper, we introduce the concept of "find the rocks, and the fluids will follow." The premise of this organizing principle is that rather than hunting for fluid effects, we should first verify reservoir presence. Once that has been achieved, the fluid effects can be more confidently extracted from the data.

However, we do not propose that this is a silver bullet. As always, there are exceptions to the rule, and for this reason, we emphasize that there is no substitute for a thorough rock physics driven analysis. In certain circumstances, it may not be possible to create a lithology stack. Particular circumstances may mean that reservoirs will remain seismically invisible no matter what. In the Eocene interval of the North Sea, for example, over a depth range of approximately 2500–3500 ft, it is often the case that reservoirs and nonreservoirs have almost identical rock properties. This is due to the highly unconsolidated nature of the rocks. In this case, the only time reservoirs become seismically visible is when they are hydrocarbon bearing. This fortuitous-sounding result is complicated by the fact that oils at this shallow level

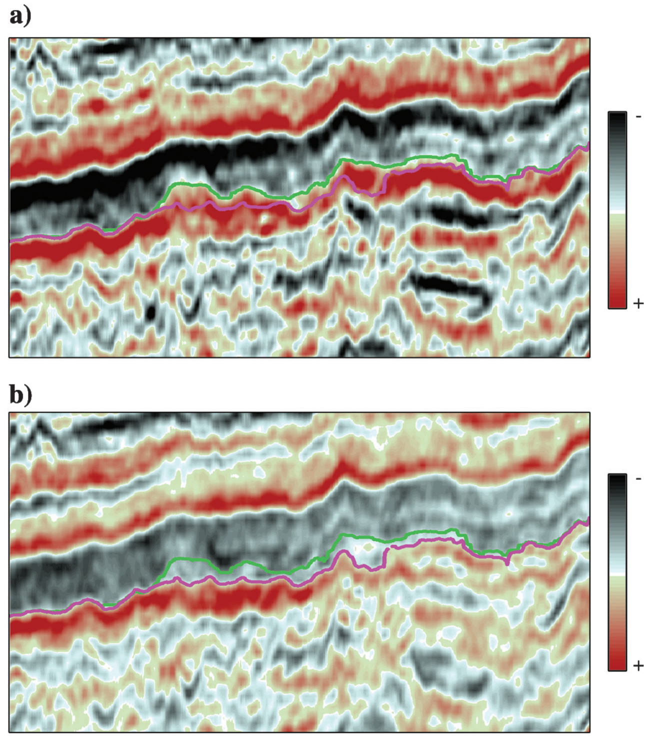

Figure 10. Relative AI and corresponding lithology impedance volume from a North Sea Paleocene prospect. The data are SEG wavelet-processed reverse polarity, where a downward increase impedance is a trough or negative number. Black colors represent soft lithologies. The interpretation of the green horizon on the upper image, RAI, would not be possible using a conventional full-stack impedance volume. The lithology volume (EEI in this example) in the lower image provides a clearer image of the reservoir, regardless of fluid fill. In this case, the response is consistent with hydrocarbon-bearing reservoir and confirmed with offset well and oil field data where an identical response is observed. Data are courtesy of CGG and E.On UK.

are often biodegraded and low API, giving rise to quite subtle fluid effects. In certain situations, rock properties can change very rapidly over small depth ranges, making the generation of a lithology volume very difficult because the AVO character of the reservoir can change quite dramatically with depth. However, even in this case, progress can be made with depth trend analysis using offset well data to analyze possible scenarios. Of course, one should always ensure that the seismic data are of sufficient quality to perform AVO-based work, by performing QC as outlined earlier in this paper.

For some, the idea that the full stack on which they have been interpreting for many years may not be showing reliable structure can be a difficult to take on board. This concept, therefore, requires analysis and testing — which can be readily demonstrated by modeling, inversion, and case studies.

In frontier areas, there is always a great deal more uncertainty in AVO analysis. However, the underlying principles of the technique can be carefully used to provide lithology and fluid information. One such way is to rotate the seismic data (e.g., I/G or Rp/Rs etc.) to the minimum reflectivity angle. Lithological contrasts provide most of subsurface reflectivity and are laterally and

a)

b)

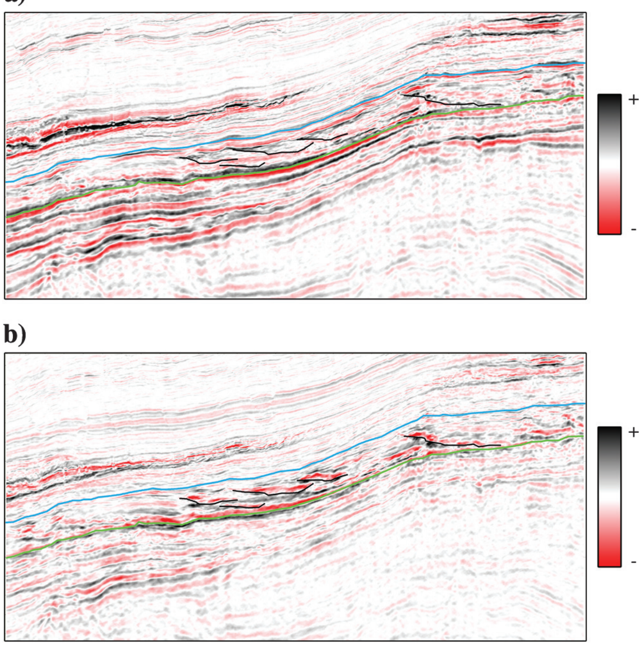

Figure 11. Relative AI (a) and corresponding lithology impedance (b) over a stratigraphic prospect West Africa. Data are SEG wavelet-processed normal polarity, where a downward increase in impedance is a peak. Blue colors therefore represent hard layers. The channel complex is clearly illuminated by the lithology volume between the blue and green horizons, while at the same time suppressing other high reflectivity events that are not related to reservoir presence. This allows for a more focused interpretation effort. In this case it would be difficult (if not impossible) to map the reservoirs using AI because, as is shown by comparison of the lithology and AI data (see solid lines), the reservoirs appear as hard and soft AI layers.

vertically extensive. By rotating the data and computing rms amplitude from the rotated products in the window of interest, it is usually possible to determine an angle that minimizes the lithological overprint. This angle will, by definition, highlight fluid effects if the seal/reservoir reflectivities do not lie on the same projection angle as the hydrocarbon reservoir properties (as outlined in the paper after Whitcombe et al. [2001] and as described in Figure 4). By rotating to an approximate orthogonal angle, lithological effects can be maximized. Further careful analysis of intermediate angles (typically close to the fluid angle) may yield the porosity angle, referred to earlier in this paper. While this workflow is more uncertain due to the paucity of control wells, this has proven to be a robust approach in areas with little or no well control. However, it is advised that the interpreter inspect maps of the reservoirs at many angles to ensure that spatially realistic geologic geometries are observed and that there is consistency to the underlying geologic and geophysical play concepts. The final selection of angles should, where possible, be verified by modeling using geologically and geophysically reasonable analogues.

The generation of lithology and fluid stacks requires careful selection of the seismic processing sequence. Where data are poorly processed, contain large errors in offset-angle conversion or contain residual NMO, artifacts may arise. These may appear as hummocks and swales in the data, or very large amplitudes — Hot spots. In these cases, the lithology volume may require combination with a more robust structural stack.

The benefits of interpreting on lithology volumes (e.g., a volume that shows sand/shale or carbonate/shale) are clear. A lithology volume simplifies the interpretation process by allowing the interpreter to focus on a single stack rather than many different stacks. They provide a robust, objective framework for lithostratigraphic interpretation and can be calibrated to offset wells when available. They are conceptually simple, repeatable, and transferable between disciplines. Once the lithostratigraphic interpretation is completed, the fluid volume can be used with confidence to discriminate between brine and hydrocarbons within the reservoirs.

Conclusions

With recent advances in seismic acquisition and processing (AVO friendly and amplitude preserving) as well as poststack denoising techniques (e.g., frequency slice filtering, or other variations thereof), the benefits of interpreting on lithology reflectivity or (relative) impedance volumes far outweigh those of using, e.g., full stack alone. A lithology stack is a stack, which shows primarily lithological variations, with the effects of fluid variations much suppressed — Depending on the case at hand, it might be a near-angle stack, a weighted sum of two angle stacks, a derived AVO reflectivity product, or a relative impedance from an inversion process (here, we typically avoid the use of absolute inversion products on the basis that a priori information about lithology, aka the low-frequency model, still has to be defined). Simple stacks that can be generated from prestack data might be S-reflectivity (often derived using AVO approximations), gradient (from a two or three-term AVO fit), Mu reflectivity, or a projection to a far-offset or chi angle reflectivity. The selection of the lithology stack should be based on modeling, which should include a review of the noise content of the seismic data.

In addition to the above list of litho stacks, we can also derive fluid stacks, which are designed to be as sensitive as possible to pore-fill. These are typically inspected and analyzed after the litho stacks have been interpreted.

In recent years, AVO has been used increasingly (and often with great success) during exploration and field production scenarios to identify and track fluid, pressure and temperature changes in the subsurface, to optimize placement of exploration and production/in-fill drilling locations. Pivotal to the success of these techniques is the identification and mapping of discrete reservoir units, by the use of lithology volumes.

Acknowledgments

We wish to acknowledge E.On UK, CGG, Canadian Overseas Petroleum Limited (COPL), Apache Corp, Tullow Oil PLC and partners, and GXT for permission to publish the images in this paper.

References

Aki, K., and P. G. Richards, 1980, Quantitative seismology: Theory and methods: W. H. Freeman and Co.

Avseth, P., J. Dvorkin, G. Mavko, and J. Rykkje, 2000, Rock physics diagnostics of North Sea sands: Link between microstructure and seismic properties: Geophysical Research Letters, **27**, 2761–2764, doi: 10.1029/1999GL008468.

Avseth, P., T. Mukerji, and G. Mavko, 2005, Quantitative seismic interpretation: Cambridge University Press.

Batzle, M., and Z. Wang, 1992, Seismic properties of pore fluids: Geophysics, **57**, 1396–1408, doi: 10.1190/1.1443207.

Connolly, P. A., 1999, Elastic impedance: The Leading Edge, **18**, 438–452, doi: 10.1190/1.1438307.

Connolly, P. A., 2010, Robust workflows for seismic reservoir characterization: SEG Distinguished Lecture Tour.

Fatti, J. L., G. C. Smith, P. J. Vail, and P. R. Levitt, 1994, Detection of gas sandstone reservoirs using AVO analysis: A 3-D seismic case history using the geostack technique: Geophysics, **59**, 1362–1376, doi: 10.1190/1.1443695.

Gardner, G. H. F., L. W. Gardner, and A.R. Gregory, 1974, Formation velocity and density — The diagnostic basics for stratigraphic traps: Geophysics, **39**, 770–780, doi: 10.1190/1.1440465.

Gassmann, F., 1951, Über die elastizität poröser medien: Veirteljahrsschrift der Naturforschenden Gesellschaft in Zurich, **96**, 1–23.

Greenberg, M., and J. P. Castagna, 1992, Shear wave velocity estimation in porous rocks: Theoretical formulation, preliminary verification and applications: Geophysical Prospecting, **40**, 195–209, doi: 10.1111/j.1365-2478.1992.tb00371.x.

Han, D., and M. Batzle, 2000, Velocity, density and modulus of hydrocarbon fluids — Empirical modeling: 70th Annual International Meeting, SEG, Expanded Abstracts, 1862–1866.

Hashin, Z., and S. Shtrikman, 1963, A variational approach to the elastic behavior of multiphase materials: Journal of the Mechanics and Physics of Solids, **11**, 127–140, doi: 10.1016/0022-5096(63)90060-7.

Jones, I. F., R. Christensen, J. Haynes, J. Faragher, I. Novianti, H. Morris, and G. Pickering, 2004, The Brenda field development: A multi-disciplinary approach: First Break, **22**, 85–91.

Kuster, G. T., and M. N. Toksoz, 1974, Velocity and attenuation of seismic waves in two-phase media, Part I: Theoretical formulations: Geophysics, **39**, 587–606, doi: 10.1190/1.1440450.

Lancaster, S., and D. Whitcombe, 2000, Fast-track "colored" inversion: 70th Annual International Meeting, SEG, Expanded Abstracts, 1572–1575.

Mavko, G., T. Mukerji, and J. Dvorkin, 1998, The rock physics handbook: Tools for seismic analysis of porous media: Cambridge University Press.

Min-Hoe, L., K. Waters, H. D. Johnson, and C. A. L. Jackson, 2008, Prospecting and modeling the deep water turbidite through integrated G&G studies: Presented at International Petroleum Technology Conference, SPE.

Ross, C. P., and P. L. Beale, 1994, Seismic offset balancing: Geophysics, **59**, 93–101, doi: 10.1190/1.1443538.

Sams, M. S., and T. Focht, 2013, An effective inclusion-based rock physics model for a sand–shale sequence: First Break, **31**, 61–71, doi: 10.3997/1365-2397.2013007.

Simm, R., 2007, Practical Gassmann fluid substitution in sand/shale sequences: First Break, **25**, 61–68, doi: 10.3997/1365-2397.2007030.

Smith, G. C., and P. M. Gidlow, 1987, Weighted stacking for rock property estimation and detection of gas: Geophysical Prospecting, **35**, 993–1014, doi: 10.1111/j.1365-2478.1987.tb00856.x.

Thomas, E. C., and S. J. Stieber, 1975, The distribution of shale in sandstones and its effect upon porosity: Presented at Sixteenth Annual Logging Symposium, SPWLA.

Waters, K., 2012, Regional rock physics for exploration in the West of Shetlands: 74th Annual International Conference and Exhibition, EAGE, Extended Abstracts, C008.

Whitcombe, D., and J. G. Fletcher, 2001, The AI-GI cross plot as an aid to AVO analysis and calibration: 71st Annual International Meeting, SEG, Expanded Abstracts, 219–222.

Whitcombe, D. N., 2002, Elastic impedance normalization: Geophysics, **67**, 60–62, doi: 10.1190/1.1451331.

White, R. E., 1980, Partial coherence matching of synthetic seismograms with seismic traces: Geophysical Prospecting, **28**, 333–358, doi: 10.1111/j.1365-2478.1980.tb01230.x.

Wyllie, M. R. J., 1963, The fundamentals of well log interpretation: Academic Press Inc.

Wyllie, M. R. J., A. R. Gregory, and L. W. Gardner, 1956, Elastic wave velocities in heterogeneous and porous media: Geophysics, **21**, 41–70, doi: 10.1190/1.1438217.

Zoeppritz, K., 1919, Erdbebenwellen VIIIb, Über reflexion und durchgang seismischer wellen durch unstetigkeitsflächen: Goettinger Nachrichten, **1**, 66–84.

References general reading

Gray, D., 2002, Elastic inversion for Lame parameters: 72nd Annual International Meeting, SEG, Expanded Abstracts, 213–216.

Naeini, E. Z., and H. Morris, 2012, Novel noise reduction for time-lapse and AVO workflows: First Break, **30**61–66.

Shuey, R. T., 1985, A simplification of the Zoeppritz equations: Geophysics, **50**, 609–614, doi: 10.1190/1.1441936.

Whitcombe, D., and L. Hodgson, 2007, Stabilizing the low frequencies: The Leading Edge, **26**, 66–72, doi: 10.1190/1.2431833.

Whitcombe, D. N., P. A. Connolly, R. L. Reagan, and T. C. Redshaw, 2002, Extended elastic impedance for lithology and fluid prediction: Geophysics, **67**, 63–67, doi: 10.1190/1.1451337.

Kester D. Waters is a geoscientist with over 10 years experience in geology, geophysics and petrophysics. Since joining Ikon Science in 2004, he has been involved in over 200 interpretation projects spanning many of the world's oil and gas producing sedimentary basins. During this period, he has been actively involved in both operational and non-operational aspects of exploration and development drilling, determining workflows and techniques for the integration of geological and geophysical data and developing predictive models for drilling risk reduction. Since 2010 he has managed an international team of geoscientists working on a variety of rock physics, inversion and AVO focused projects across the Europe, Africa and Middle Eastern regions and has been a driving force behind the on-going development of Ikon Science's RokDoc® software platform. In 2013, he became product owner of Ikon Science's 3D reservoir characterisation software, responsible for its on-going and future development. He has an M.S. in Geology from Liverpool University, UK and an M.S. in Petroleum Geoscience from the University of Aberdeen, UK.

Michel A. C. Kemper is a geoscientist with 26 years of experience in geophysics, petrophysics, and reservoir engineering. The first 13 years were spent with Shell International in the Hague, Nigeria, and London, during which he made contributions to the interface between petrophysics and geophysics. In 1999, he became team leader in petrophysics/petroacoustics at Ikoda Limited, working on a wide variety of projects. It is during this time that RokDoc — now one of Ikon Science's main products — was started. He was one of the cofounders of Ikon Science and now he is the Director of Technology, Research & Development, responsible for the incorporation of latest techniques and developments in the area of rock physics into the Ikon Science software portfolio.